

INFLUENCE OF LOCAL VERSUS GLOBAL IONOSPHERIC MODEL ON PRECISE GPS POSITIONING

Ali Ahmed ElSagheer¹, Maher Mohamed Amin², Farag Bastawy Farag², Khaled Mahmoud Abdel Aziz²

¹Dean, Faculty of Engineering, Nahada University,

²Benha University, Shoubra Faculty of Engineering, Department of Surveying Engineering (EGYPT)

E-mails: alielsagheer@yahoo.com, dr_maher_amin@yahoo.com,
dr.farag.7@hotmail.com, khaledmahmoud81@yahoo.com

DOI: 10.7813/2075-4124.2014/6-4/A.20

Received: 16 Feb, 2014

Accepted: 17 Jun, 2014

ABSTRACT

The ionosphere is one of several layers of the Earth's atmosphere. The influence of the ionosphere on GPS positioning is one of the largest error sources. It is generally modeled in a global scale by determining its Total Electron Content (TEC) in the signal path using all available world wide GPS observations to be used in GPS processing procedure to overcome its error, the modeled product is known as Global Ionospheric Model (GIM). In this research, a Local Ionosphere Model (LIM) was created using Bernese software, by the computation of TEC in a local area. This process was based on the single layer model to determine the appropriate TEC values by using the Egyptian coastal part composed of five stations of the network made by the Egyptian National Research Institute of Astronomy and Geophysics (ENRIAG) at (2001). The influence of using the global ionospheric model versus the obtained local model was investigated, with precise ephemeris, for different base line lengths, and different observational sessions (1, 2, 3, 4, 5 and 6 hours), based on the commercial software Trimble Total Control (TTC). Additionally, the influence of the Precise Ephemeris (PE) alone without using ionospheric models was also studied for the same base line lengths, and the same observation sessions based on the same commercial software. The results indicate that the mean of vector length errors was improved when using the (LIM) with precise ephemeris, at all different baseline lengths and also with different observational sessions.

Key words: Bernese GPS software version 5.0, Trimble Total Control (TTC) software version 2.7, Precise Ephemeris, Precise GPS positioning, Global ionospheric Model (GIM) and Local Ionospheric Model (LIM)

1. INTRODUCTION

The atmosphere is a relatively thin layer of gases (air) and dust surrounding the Earth. The interaction of particles in the atmosphere affects the propagation of GPS signals due to refraction. To describe this phenomenon we may think the atmosphere as composed of two parts. The first part contains charged particles or ionized particles (ionosphere), where the essential effects on the signals are occurred. The second part is composed only of non ionized particles (troposphere), where charged particles are practically absent [7].

GPS observations are known to be contaminated by different kinds of errors; such errors are due to satellites, the receivers and the medium through which the signals pass. Some of these errors are usually eliminated or reduced through differencing between the satellites or between the receivers [5].

The atmosphere surrounding the earth surface causes the signals passes through this medium to be delayed especially when it passes through the ionosphere. This part of the atmosphere contains charged particles that have different behavior and causes the signals to be refracted and thus delayed. This medium is considered the main error's source of GPS observation. It is generally modeled in a global sense based on global GPS observations giving what is called GIM.

In commercial GPS works where required accuracy is limited the PE is usually used alone in processing, while in precise GPS works GIM with PE are used for the same purpose. For more accurate result of GPS we have tried in this research to create a LIM based on permanent GPS stations in the local investigation area to be used with PE in processing procedure. To check the proposed idea, a comparison has been made between the results of the three processing procedures of GPS observations using the PE alone, GIM with PE and LIM with PE. The final results of the comparison have proved the merit of using LIM with PE over using the other two.

2. STUDY AREA, AND DATA SOURCES

In this research, the created local ionospheric model was accomplished by analyzing the dual-frequency GPS data from five stations of the ENRIAG network which lies on the north coastal part. The network covers approximately an area from 30° 52' N to 31° 15' N in latitude and from 27° 14' E to 33° 38' E in longitude, see Figure (1).



Fig. 1. A coastal Part of the Egyptian National Earthquakes Network.

Where the following data were collected for the computations:

- Twenty-four hours GPS data at a rate of one-second in RINEX format for the five stations MNSR, SAID, BORG, ARSH, and MTRH were obtained from ENRIAG for one Day of the Year (DoY) 018/2013, and the precise point positioning for MNSR Station (Fixed coordinates).
- Precise satellite ephemeris (final orbits) data for GPS week 1723 were downloaded from the International GNSS Service (IGS) Day of Year (DoY) 018/2013.
- Global Ionospheric Model (GIM) which was generated every two hours starting from 0 to 24 hours at same day was downloaded.

3. METHODOLOGY

3.1 Extracting Ionospheric Information from GPS Observations

The ionosphere is a dispersive medium for radio waves; it produces an advance in carrier phase observations and a delay in code observations. The magnitude of the advance/delay in meters caused by the ionosphere is given in equations 4 and 5, where the '+' sign is used for code observations and the '-' sign is used for phase observations [4]. This means that the measured code pseudo-range is too long and the measured phase pseudo-range is too short, when compared to the actual geometric distance between the satellite and the receiver [1].

One of the problems for all space geodetic techniques operating with electromagnetic waves is the determination of the propagation velocity of the signals. If these waves propagated in vacuum, the traveled distance would be just the product of the propagation time between emitter and receiver and the speed of light in vacuum. When signals travel through the ionosphere, the interaction between the electromagnetic field and the free electrons influences both the speed and the propagation direction of the signal, an effect known as ionospheric refraction [2].

The ratio between the propagation speed (c) of a wave in vacuum and the propagation speed (v_{ph}) in a given medium is known as the refractive index (n):

$$n = \frac{c}{v_{ph}} \quad (1)$$

The Appleton-Hartree theory allows the calculation of the refractive index for a single wave, which propagates through plasma (ionized medium) [6].

The approximate expression for the refraction coefficient n_{ph} for carrier phase observations:

$$n_{ph} = 1 - \frac{40.3N_e}{f^2} \quad (2)$$

Where f^2 the carrier frequency is expressed in Hertz and N_e is the free electron density in the medium. Notice that the coefficient 40.3 contains several constant parameters including their dimensions.

The refraction coefficient for the pseudorange measurement n_g is of the same size but opposite sign:

$$n_g = 1 + \frac{40.3N_e}{f^2} \quad (3)$$

Note that n_g is expressed as a group index (a wave group generated by superposition of different waves of different frequencies), as opposed to phase index n_{ph} of a particular wave with constant wavelength [8].

Now we can calculate the carrier phase delay d_{ph} to obtain the influence of the ionized medium on the propagated wave

$$d_{ph} = \int_s (n_{ph} - 1) ds = -\frac{40.3}{f^2} \int_s N_e ds = -\frac{40.3 \cdot 10^{16}}{f^2} STEC \quad (4)$$

The integral of the electron density along the signal path S is usually called STEC (Slant Total Electron Content). This quantity can be interpreted as the total amount of free electrons in a cylinder with a cross section of $1m^2$, of which the axis is the slant signal path. STEC is measured in Total Electron Content Units (TECU), which is equivalent to 10^{16} electrons/m². The effect of the ionized medium on group propagation can be expressed by:

$$d_g = \int_s (n_g - 1) ds = \frac{40.3}{f^2} \int_s N_e ds = \frac{40.3 \cdot 10^{16}}{f^2} STEC \quad (5)$$

The last two expressions show how the electron content in the ionosphere can influence measurement's ranging from outer space to Earth-based stations. If the behavior of the ionosphere is known, these effects can be computed and used to correct measurements on radio frequencies. If ionospheric parameters are not available, observing at two different radio frequencies allows the elimination of most ionospheric influences [6].

3.2 Global Ionospheric Models (GIM)

From the (GIM) which is made, on a daily basis each 5° in longitude and 2.5° in latitude, at the International GNSS Service and other institutions, the final Global Ionospheric corrections are obtained [9].

3.3 Local Ionosphere Modeling Derived by the Bernese-Software

3.3.1 Deterministic Component

Global Navigation Satellite Systems (GNSS) -derived ionosphere models describing the deterministic component of the ionosphere are usually based on the so-called Single-Layer Model (SLM) as illustrated in figure (2) [10].

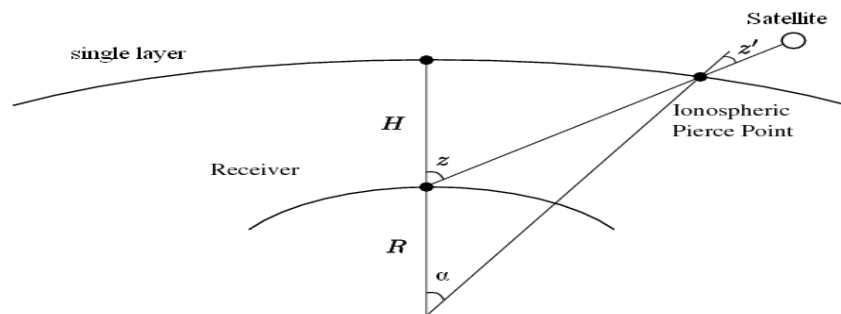


Fig. 2. Geometry of the Single-Layer Ionospheric Model [After, 3]

It assumes that all free electrons are concentrated in a shell of infinitesimal thickness. The height H of this idealized layer above the Earth's surface is usually set to be the expected height of the maximum electron density. In most of the IONEX solutions H is set to be 450 km.

The SLM mapping function F , which is used for the transformation between VTEC and STEC:

$$STEC = F(Z) \cdot VTEC \quad (6)$$

Where:

$$F(Z) = \frac{1}{\cos z'} \quad \text{with} \quad \sin z' = \frac{R}{R+h} \sin z \quad (7)$$

And;

z, z' are the zenith distances at the height of the station and the single layer, respectively figure (2),

R is the mean radius of the Earth, and

H is the height of the single layer above the Earth's surface [6].

The "modified" SLM (MSLM) mapping function includes an additional constant, α :

$$F(Z) = \frac{1}{\cos z'} \quad \text{with} \quad \sin z' = \frac{R}{R+h} \sin(\alpha z) \quad (8)$$

For estimating VTEC, the geometry-free linear combination L4 was used which principally contains the ionospheric delay and the initial phase ambiguities. The same linear combination may be formed using the code observations too.

$$L_4 = L_1 - L_2 \quad (9)$$

The particular observation equations for un-differenced phase observation read as:

$$L_4 = -a \left(\frac{1}{f_1^2} - \frac{1}{f_2^2} \right) F(Z) E_v(\beta, S) + B_4 \quad (10)$$

Where

L_4 are the geometry-free phase observables (in meters),

$a = 4.03 \cdot 10^{17} \text{ ms}^{-2} \text{ TECU}^{-1}$ is a constant,

f_1, f_2 are the frequencies associated with the carriers L1 and L2,

$F(z)$ is the mapping function evaluated at the zenith distance z' ,

$E_v(\beta, s)$ is the vertical TEC (in TECU) as a function of geographic or geomagnetic latitude β and sun-fixed longitude s , and

$B_4 = \lambda_1 B_1 - \lambda_2 B_2$ is a constant bias (in meters) due to the initial phase ambiguities B_1 and B_2 with their corresponding wavelengths λ_1 and λ_2 [10].

3.3.1.1. Local VTEC Model

For the determination of the parameters of local VTEC, a spherical harmonics expansion (11) was used. This equation is also used for regional or global applications, depending on the extent of the considered area and the distribution of the observational stations.

$$E_v(\beta, s) = \sum_{n=0}^{n_{\max}} \sum_{m=0}^n \tilde{P}_{nm}(\sin \beta) (\tilde{C}_{nm} \cos(ms) + \tilde{S}_{nm} \sin(ms)) \quad (11)$$

where:

β is the geographic or geomagnetic latitude of the intersection point of the line of sight with the single layer,

$s = \Lambda - \Lambda_0$ is the sun-fixed longitude of the ionospheric pierce point,

Λ is the longitude of the ionospheric pierce point,

Λ_0 is the longitude of the sun,

$\tilde{P}_{nm} = N_{nm} P_{nm}$ is the normalized associated Legendre function of degree n and order m ,

$N_{nm} = \sqrt{\frac{(n-m)!(2n+1)}{(n+m)!}}$ is the normalization function,

P_{nm} is the conventional Legendre function,

n_{\max} is the maximum degree of the spherical harmonics expansion,

$\tilde{C}_{nm}, \tilde{S}_{nm}$ are the (unknown normalized) TEC coefficients of the spherical harmonics, i.e., the ionospheric model parameters to be estimated [6].

4. PRACTICAL WORK

In commercial GPS works the PE is usually used alone in processing, which produce a limited degree of position accuracy, while in precise GPS works GIM with PE instead are used together for the same purpose. In this section a LIM has been created based on the available five permanent GPS stations laying on the local area of the northern part of Egypt against the Mediterranean sea to be used together with the PE in processing, hoping to get more accurate results. The same can be reproduced in future every day in the same local area whenever local data are available. The comparisons of the final results after the three processing procedures have proved the merit of using LIM with PE over the other two (PE alone and PE with GIM).

The LIM of the study area has been created according to following steps:

- The MNSR station was the only fixed station available to us. This station was used through baselines to fix the remaining four stations (SAID, BORG, ARSH, and MTRH) by processing the available 24 hours observations at these stations using Bernese software. This software was design to create the GIM each 2 hours with grid nodes of 5° in longitude and 2.5° in latitude based on the available 24 hours observations at globally distributed stations. To create the required LIM our job was mainly to modify the Bernese global grid to a finer grid mesh comparable with our small local test area. Our trials had shown that the perfect resolution to be used should depend on the actual separation between the stations; i.e the resolution should be smaller as long as the separation is lesser and vise versa. That's why in our study area we were obliged to make two LIMs, each has its own resolution, due to the variation of the separation between the stations; which were categorized into two groups, figure (1).

- The first LIM, based on shorter baselines between stations (MNSR, SAID and ARSH), was created with resolution of 30 minutes in longitude and 10 minutes in latitude based on the 24 hours observations at the mentioned five stations to produce a LIM every 10 minutes time, which was found to be the minimum time that gives the optimum correction of the LIM. A Single Layer Model (SLM) of height (H) equal 450 km was used for modeling the vertical total electron content (VTEC) using the geometry-free linear combination (L4). This LIM was found suitable for the limited local area between ARSH and MANS, but not suitable for the area from MNSR and MTRH where baselines were greater there, that is why we have made another LIM for the second area with bigger resolution of 2.5 degree in longitude and 30 minutes in latitude each 10 minutes time using the same procedure of creating the first LIM. A small subroutine has been made and added to the Bernese software for this purpose.
- To check the impact of using the obtained LIM on the accuracy of the computed coordinates, we have used the 24 hours RINEX data with a 1 second sampling rate at the five stations. The processing had been made with Trimble Total Control (TTC) software, to find the coordinates at different observational sessions (1h, 2h, 3h, 4h, 5h and 6 hours) by using precise ephemeris (IGS final orbits) with or without ionosphere models (GIM or LIM).
- The mean of vector length error (Δs) at each station was computed by subtracting the coordinates obtained by Trimble Total Control (TTC) software at different observational session from its fixed one obtained from step 1.
- Certain precautions had been taken to determine the true mean value of vector length errors to exclude any blunder observation from the whole set of observation, due to the (DOP) that exceeds 6; bad observation at afternoon hours and/or observation at night, when dramatic instability of the ionosphere resulted from remerging of electrons and ions, during the different sessions.

5. RESULTS

Table (1) demonstrates the relative accuracy for the three GPS orders of survey network stations [11]. Table (2) present the minimum time of baseline solution per km [12].

Table 1. Specifications of Relative Accuracies for Various GPS Survey

Order	Distance Accuracy	Relative Accuracy	Purpose
A 1 st	0.5 cm	0.1 ppm	US Geodetic Reference Network, Earth Surface Deformation
B 2 nd	0.8 cm	1.0 ppm	Local Earth Surface Deformation, High Accuracy Engineering Surveying
C 3 rd	1.0 cm	10 ppm	Engineering Surveying, Urban Control Surveying

Table 2. Typical Static Observation Times for Baseline Solution

Length of Baseline	Minimum Observation Time
Less than 10 km	45 minutes
10 to 40 km	1 hour
40 to 100 km	2 hour
100 to 200 km	3 hour
More than 200 km	4 hour or more

Tables (3) through (8) show the results of the mean vector length errors (Δs) at each of the five stations, using the three different processing procedures.

Table 3. Mean of Vector Length Errors (Δs) at SAID Station Using the Three Processing Procedure and MNSR-SAID Base Line Whose Length is 94.477 km.

Time	PE only (Δs)	GIM + PE (Δs)	LIM + PE (Δs)
1h	14.00 cm	4.0 cm	2.0 cm
2h	08.60 cm	1.8 cm	1.9 cm
3h	10.30 cm	2.2 cm	2.2 cm
4h	04.70 cm	1.8 cm	1.8 cm

Table 4. Mean of Vector Length Errors (Δs) at ARSH Station Using the Three Processing Procedure and MNSR-ARSH Base Line Whose Length is 216.196 km.

Time	PE only (Δs)	GIM + PE (Δs)	LIM + PE (Δs)
1h	19.9 cm	11 cm	10.5 cm
2h	18.0 cm	5.1 cm	3.4 cm
3h	14.7 cm	4.3 cm	3.9 cm
4h	12.3 cm	4.9 cm	2.9 cm
5h	16.4 cm	4.1 cm	3.0 cm

Table 5. Mean of Vector Length Errors (Δs) at BORG Station Using the Three Processing Procedure and MNSR-BORG Base Line Whose Length is 171.110 km.

Time	PE only (Δs)	GIM + PE (Δs)	LIM + PE (Δs)
1h	21.1 cm	10.9 cm	7.8 cm
2h	16.9 cm	8.4 cm	4.2 cm
3h	15.3 cm	3.8 cm	3.0 cm
4h	17.6 cm	4.4 cm	3.7 cm
5h	21.5 cm	3.0 cm	2.9 cm
6h	14.2 cm	4.5 cm	3.5 cm

Table 6. Mean of Vector Length Errors (Δs) at BORG Station Using the Three Processing Procedure and ARSH-BORG Base Line Whose Length is 387.073 km.

Time	PE only (Δs)	GIM + PE (Δs)	LIM + PE (Δs)
2h	29.8 cm	12.2 cm	10.9 cm
3h	30.9 cm	8.4 cm	7.2 cm
4h	30.7 cm	6.5 cm	6.5 cm
5h	27.4 cm	12 cm	7.1 cm
6h	42.9 cm	4.3 cm	6.9 cm

Table 7. Mean of Vector Length Errors (Δs) at MTRH Station Using the Three Processing Procedure and MNSR-MTRH Base Line Whose Length is 394.245 km.

Time	PE only (Δs)	GIM + PE (Δs)	LIM + PE (Δs)
2h	29.5 cm	18.8 cm	19.8 cm
3h	21.4 cm	18.8 cm	15.8 cm
4h	32.0 cm	15.9 cm	19.1 cm
5h	29.8 cm	12.0 cm	16.0 cm
6h	31.6 cm	23.8 cm	7.60 cm

Table 8. Mean of Vector Length Errors (Δs) at MTRH Station Using the Three Processing Procedure and ARSH-MTRH Base Line Whose Length is 608.740 km.

Time	PE only (Δs)	GIM + PE (Δs)	LIM + PE (Δs)
2h	36.7 cm	29.9 cm	28.4 cm
3h	31.6 cm	23.8 cm	25.7 cm
4h	35.9 cm	21.2 cm	21.6 cm
5h	34.6 cm	17.9 cm	17.6 cm
6h	34.9 cm	28.3 cm	17.3 cm

- The results of table (3) deal with baseline less than 100 km. It demonstrates that the third processing procedure, i.e LIM with PE need only one hour to reach closely the accuracy of the first order survey network as given in table (1).
- From the same table (3) we can conclude that the second procedure, i.e GIM with PE gives the same result as the third procedure in two hour processing, while the first procedure i.e PE alone is improving each extra processing hour.
- From tables (4) and (5) the accuracy obtained from the third procedure for baselines around to 200 km length, reaches close to the first order survey network accuracy, in processing time of two hours and is always better than the other two procedures in all processing sessions.
- Tables (6) and (7) demonstrate that the two baselines ARSH-BORG and MNSR-MTRH are approximately equal in length and both are less than 400 km. Two CORS stations lies in between the end points of the first baseline, while one CORS station exists only between the end points of the second baseline. It seems that the extra point of the first case increases the accuracy of the created second LIM in this area.
- Table (8) shows that the third processing procedure for the baseline ARSH-MTRH, which has length of 608.740 km is almost better than the other two procedures in different processing sessions.

6. CONCLUSION

From the results of this research, the following conclusions can be drawn:-

- In this research two local models were created, due to the irregular baseline lengths between the network stations, in the study area.
- The results assured that using precise ephemeris with ionospheric models either local or global is much better than using precise ephemeris alone, for all baselines and for all different observational sessions.

- Based on the fourth step of the results, the accuracy of the created LIM is increased as long as the number of CORS stations used in its creation is increased.
- It is preferable to exclude afternoon hour's observations because the TEC during this period reaches its maximum.
- To reach accuracy comparable with the accuracy of the first order network in two hours, the distance between the CORS station used to create the LIM should be within 200 km.
- In general the accuracy is improved for different baseline lengths with the least observational time when using LIM in processing procedure.

7. RECOMMENDATIONS FOR FUTURE WORK

- This test should be repeated with the seasonal variations to study the effect of the ionosphere delay along the year.
- Repeating the test using data taken from other positioning satellite systems such as GLONASS, Galileo, and Compass to create the LIM.
- CORS stations used in this test area were all closely laying along the Mediterranean Sea shore, where the weather is non-dry. Another set of CORS stations is needed in the desert area to compare the effect of the dry and non-dry areas on creating the LIM.
- The LIM should be tested for accuracy of the PPP (Precise Point Positioning) to find the effect of the ionosphere only on GPS measurements and the minimum required session of observational time.
- In case enough and well distributed CORS stations all over the area of the Egyptian territory are available; the same methodology can be used to create a regional ionospheric model for the same area.

ACKNOWLEDGEMENTS

I would like to express my deep gratitude to the staff of the National Research Institute of Astronomy and Geophysics (NRIAG) in Egypt for providing me the data of GPS/CORS network and for enabling me to using the GPS processing programs.

REFERENCES

1. Hong C., (2007). Efficient Differential Code Bias and Ionosphere Modeling and Their Impact on the Network-Based GPS Positioning, Ph.D. thesis, The Ohio State University, 2007.
2. Boehm J., Hobiger.T, Schuh.H.,(2004). VLBIIONOS- Probing The Ionosphere By Means Of Very Long Baseline Interferometry, Institute of Geodesy and Geophysics, University of Technology, Vienna. Vienna, Gußhausstraße 27-29, A-1040 Wien, Austria.
3. McFadden R., Ekers R., Bray J. (2013). Ionospheric propagation effects for UHE neutrino detection with the lunar Cherenkov technique. Available at: <http://inspirehep.net/record/1236583/plots>. last accessed on: 22/6/2014.
4. Julia Talaya i Lopez (2003). Algorithms and methods for robust geodetic kinematic positioning, Barcelona: Institut cartogràfic de Catalunya, 2003.
5. Nahavandchi H. and A. Soltanpour., (2008). Local Ionospheric Modelling of GPS Code and Carrier Phase Observations, Norwegian University of Science and Technology, Division of Geomatics, Trondheim, Norway, July 2008.
6. Todorova S., Hobiger T., Weber R., Schuh H. (2003). Regional Ionosphere Modelling With GPS and Comparison With other Techniques. In proceeding of: Proceedings of the Symposium "Modern Technologies, Education and Professional Practice in the Globalizing World", November 06-07, Sofia, 2003.
7. Odijk D. (2002). Fast precise GPS positioning in the presence of ionospheric delays. PhD thesis, Netherlands Geodetic Commission, Delft, November 2002, 242pp.
8. Janssen V., (2003). A Mixed-Mode GPS Network Processing Approach for Volcano Deformation Monitoring. PhD thesis, University of New South Wales, July 2003.
9. Charoenkalunyuta T., Satirapod C., Li Y. and Rizos C. (2012). An Investigation of The Effect of Ionospheric Models On Performance of Network-Based RTK GPS In Thailand, The 33rd Asian Conference on Remote Sensing, November 26-30, 2012, Pattaya, Thailand.
10. User manual of the Bernese GPS Software Version 5.0, (2007). Astronomical Institute, University of Bern, January 2007.
11. Abdallah A., (2009). Accuracy Assessment Study Of Using GPS For Surveying Applications In South Egypt, Master thesis, Civil Engineering Department- Aswan-Faculty of Engineering-South Valley University, Aswan, Egypt, 2009.
12. Skeen J., (2011). TxDOT Survey Manual: Manual Notice: 2011-1. Availablat: http://onlinemanuals.txdot.gov/txdotmanuals/ess/gps_static_surveying.htm. Last accessed: 22/6/2014.